RESEARCH PAPER

Effect of the Number of Dips on the Properties of Copper Oxide Thin Films Deposited by Sol-Gel Dip-Coating Technique

Souheila Hettal[1], Abdelouahab Ouahab[1], Saâd Rahmane[1], Ouarda Benmessaoud[1], Aicha Kater[1], and Mostefa Sayad[1,2]

* *a.ouahab@univ-biskra.dz*

[1] Laboratory of Thin Films Physics and Applications, University of Biskra, Algeria.
[2] Laboratory of New and Renewable Energies in Arid Zones, University of Ouargla, Algeria.

Received: December 2021 **Revised: February 2022** **Accepted: February 2022**

DOI: 10.22068/ijmse.2582

Abstract: *Copper oxide thin layers were prepared by sol-gel dip-coating technique. The effect of thickness on morphology, structure, optical and electrical properties was investigated in this study. Copper chloride dihydrate dissolved in methanol was used as precursor material. The scanning electron microscopy results showed more continuity in formation of the clusters and nuclei with the increase in the number of the dips. X-ray diffraction studies showed that all the films were polycrystalline cupric oxide CuO phase with monoclinic structure and grain size in the range of 30.72 - 26.58 nm. The obtained films had clear black in appearance, which was confirmed by the optical transmittance spectra. The optical band gap energies of the deposited films varied from 3.80 to 3.70 eV. The electrical conductivity of the films decreased from* 1.90×10^{-2} *to* 7.39×10^{-3} $(\Omega.cm)^{-1}$.

Keywords: *copper oxide, thickness, dip coating, morphology, structural, optical, and electrical properties.*

1. INTRODUCTION

Metal oxides are in the midst of the most fascinating classes of solids with a variety of structures, properties, and applications [1]. The copper oxide; among these oxides, exists in two stable phases namely CuO and Cu_2O with different properties [2]. An intermediate compound between the previous two, a metastable copper oxide, (Cu_4O_3) has been also re-ported [3]. The most stable one at room temperature is cupric oxide CuO with monoclinic crystal structure is an important p-type semiconductor with an optical band gap ranging from 1.2 to 1.6 eV and a high absorption coefficient [4]. Cupric oxide thin films has demon-strated a potential use in many applications, such as catalysis [5], combustion enhancement [6], corrosion protection [7], water splitting [8], lithium batteries [9], gas sensors [10] and absorber layer in solar cells [11].

Copper oxide was synthesized using various physical, electrochemical and chemical deposition techniques including sputtering [12], electro-deposition [13], spray pyrolysis [14] and sol-gel dip-coating [8, 15]. Although copper oxide thin films deposited with different soft chemistry techniques such as spray pyrolysis show good properties for most of the cited applications, the dip coating method is one of the low-cost and easy processing methods. It has attractive advantages including a nonhazardous and well suitable for deposition at low temperatures [16]. It is reported that it produces homogeneous film structure with for large area, good crystallinity, fairly good stoichiome-try and thickness, and phase purity at ambient depositions conditions [7-8, 16-18].

Copper oxide is mainly a p type semiconductor [19]. It has suitable properties for specific applica-tions such as p-n junction diodes [20], solar cells [21], gas sensors [22], and electrode materi-als for lithium batteries [23].

It is well known that the deposition techniques alter the structure and morphology the produced thin films and hence changing their physical properties.

In this study, copper oxide thin films were deposited on glass substrate by sol gel dip-coating technique. The number of dip times (number of dips) of the films were varied from one to five in order to control the thickness and the quality of the films. The influence of the thickness of the films on the main optoelectronic properties when varying number of the dips is studied and cor-related to the morphological, structural properties.

[DOI: 10.22068/ijmse.2582]

2. EXPERIMENTAL PROCEDURES

Copper chloride dihydrate ($CuCl_2$, $2H_2O$) as a precursor is dissolved in methanol (CH_3OH) with a concentration of 1.5 mol/l before putting the solution in stirrer for about 15 minutes. The final solution was heated at 45 (°C). The obtained solution was dark green without any suspension of particles. The glass substrates were cleaned using ethanol for 10 minutes followed by acetone then rinsed using deionised water and dried with an electrical drier.

The Copper chloride dihydrate ($CuCl_2$, $2H_2O$) reacts with methanol during the sol-gel pro-cess and gives copper oxide as shown by the chemical equation [24]:

$(CuCl_2, 2H_2O) + CH_3OH \rightarrow CuO + CH_3Cl + HCl + 2H_2O$

Hydrogen chloride evolves out and the remain solution ($CH_3Cl + 2H_2O$) is dried in the furnace.

The glass substrates were dipped into the solution for 5 minutes with a withdrawal speed equal to 1330 (µm/s), this process is repeated from one to five times to achieve various thicknesses. The obtained films were dried in infrared drier for 5 minutes at 100 (°C) immediately, after the drying process the thin films were annealed in furnace for 60 minutes at 500 (°C) with heating rate of 16.7 (°C/min) to further increase the crystallinity of the films. The films are left to rest in the furnace till reaching the ambient temperature in order to avoid film's cracking.

The thickness of copper oxide films was measured using the approximate gravimetric method where the weight measurement of the substrate before and after deposition by using an accurate balance. Supposing a constant and uniform density of the film's material; the surface substrate and the density values give access to the thickness using the following equation is [26]:

$$d = \frac{m}{(g*A)} \quad (1)$$

Where *g, m, and A are* the film material density, its mass, and the substrate area, respectively.

TESCAN VEGA3Scanning Electronic Microscopy (SEM) was used for analyzing surface morphology. The X-ray diffraction patterns were carried out using Rigaku-Type MiniFlex 600 with Cu Kα radiation (λ= 1.5418 Å) to identify the structure information. The grain sizes are calculated using the Scherer formula from the relevant XRD peaks of the spectrum [27]:

$$D = \frac{0.9\lambda}{\beta \cos\theta} \quad (2)$$

where D is the average size of grains in the film, λ is the X-ray wavelength (1.5418 Å), β is the full width at half maximum (FWHM) of the peak in radians and θ is Bragg's angle.

The investigation of the optical properties in the wavelength range 300- 1500 nm is achieved using a JASCO V-770 spectrophotometer. In order to determine the optical band gap energies E_g of cupric oxide of the thin dips Tauc's formula is used [24]:

$$\alpha h\upsilon = A(h\upsilon - E_g)^n \quad (3)$$

where A is a constant, E_g the semiconductor band gap and n is a number equal to 0.5 for the direct gap and 2 for indirect gap compounds. The band energies are then obtained by extrapolating the linear portion of $(\alpha h\upsilon)^2$ versus $h\upsilon$ plots to the energy axis at $(\alpha h\upsilon)^2 = 0$. The band tail states absorption due to the localized states called Urbach tails; which extend into the band edge, is calculated from the following equation [30]:

$$\alpha = \alpha_0 e^{\frac{h\upsilon}{Eu}} \quad (4)$$

Where α_0: is the pre-exponential factor, hν the photon energy and E_u is the band tail width or disorder energy. The determination of the electrical conductivity is conducted using the four-point probe measurement technique with a KEITHLEY 2400 as a source meter.

The electrical properties of the cupric oxide thin films were characterized by the four-point probe method to determine the resistivity using the following formula [30]:

$$\rho = d(\frac{\pi V}{\ln(2) I}) \quad (5)$$

Where ρ: is the resistivity, d is the film thickness, the measured V is the voltage and I is the current.

3. RESULTS AND DISCUSSION

3.1. Physical properties

The surface morphology of the copper oxide thin films was investigated by using SEM and the photographs are shown in Fig1. The magnification is taken about 5.00 kx for all the films.

It is clear that the growth of copper oxide thin films is affected by the layer's number. The first sample of 1 layer shows a covered surface with some cracks contrarily to the rest of the samples where they are completely covered.

[DOI: 10.22068/ijmse.2582]

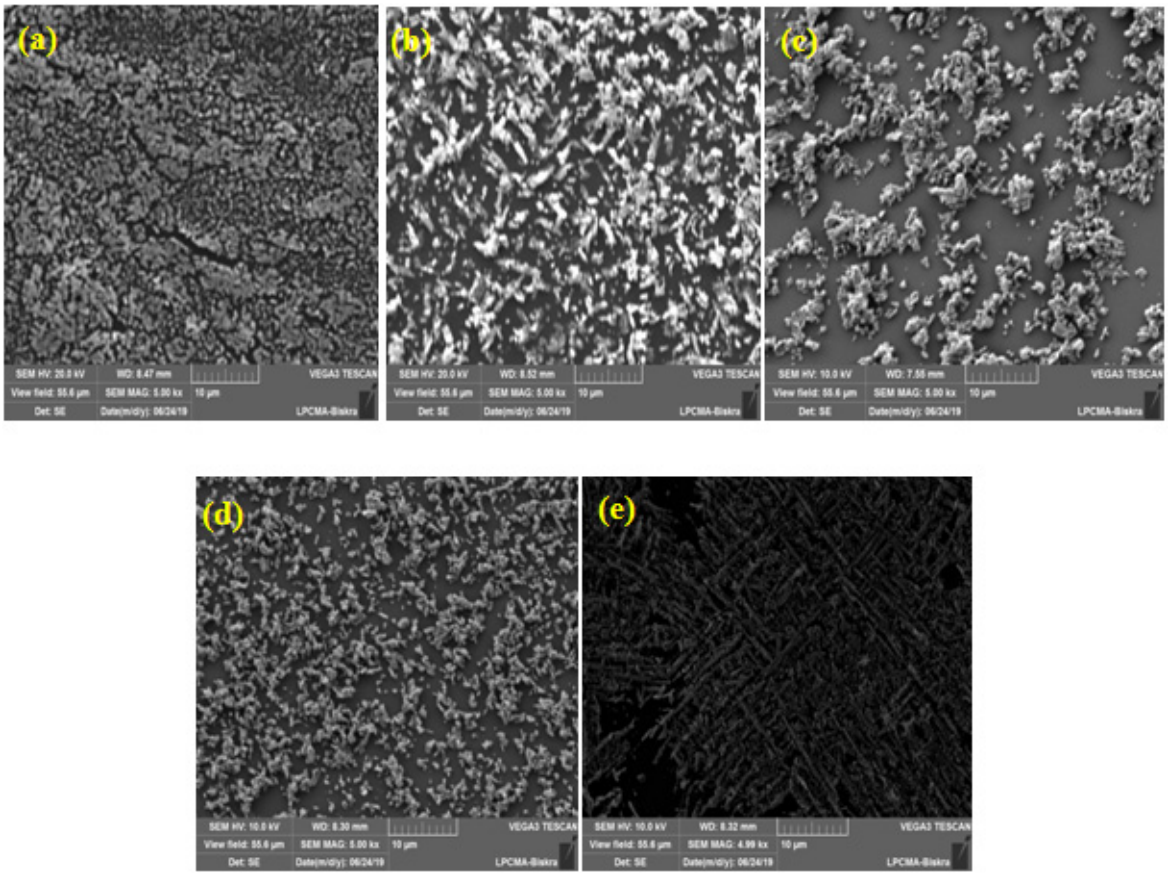

Fig. 1. SEM images for the deposited CuO dips; (a) 1 layer, (b) 2 dips, (c) 3 dips, (d) 4 dips and (e) 5 dips.

Isolated grains are also formed and change in form and density when the number of dips changes. These agglomerates increase in number and decrease in size with the increase of the thickness till the film become ho-mogenous and an amelioration (decrease) of the film roughness is gained with the number of deposited dips is evident. For the sample of containing 5 dips, the film photograph was taken near to the substrate edge and show that the film becomes denser forming a continu-ous network where the surface are free of cracks. The number of dips affects the film by adding more matter accompanied by an increase in its thickness.

In table 1, the thickness values of the deposited films with the growing num-ber of dips are listed. It can be seen that these values indicate clearly that the thickness increases with the number of the dips from the hundreds of nanometer to the micrometer range. A similar effect was reported for TiO_2 thin films [25], tin oxide [26], and for silica thin films [7]. This fact endorses the improvement of the morphology seen in the SEM mi-crographs.

Table 1. The thickness values of copper oxide CuO thin films.

Sample	Thickness (nm)
1 dip	471.04
2 dips	556.64
3 dips	764.61
4 dips	834.01
5 dips	1219.36

3.2. Structural properties

The XRD diffractograms of different films are recorded and shown in Figure 2 and it is compared with JCPDS n° 01-074-1021 for the thickness of 471.04 because it shows three peaks near to 31.80°, 35.60° and 38.75° which are matched to (110), (-111) and (111) reflec-tions of cupric oxide (CuO) respectively. The preferential orientation is the (110) for the film with one layer while for the samples with two to five dips the peak of 31.80° disap-pears completely. Compared with JCPDS card n° 01-080-1268, we found that the preferen-tial orientation becomes the (-111)

[DOI: 10.22068/ijmse.2582]

for all these samples. All the peaks of the samples reveal that the deposited films are composed of single phase CuO with monoclinic crystal structure belonging to C2/2 space group and no other related peaks refer to Cu_2O and Cu_4O_3 phases are seen. The change in the crystallographic orientation from (-111) to (111) is probably due to the change in stress within the films as the number of the dips increase, as we will see in the next paragraph.

The intensity of the peaks is significantly increasing from the sample of 1 to 2 dips and after that it decreases for the case of 3 dips sample (764.61 nm), then it increases due to the improvement of the crystallinity of the films which is in good agreement with the mor-phology of surfaces becoming denser due to the coalescence and the gathering of the ag-glomerates.

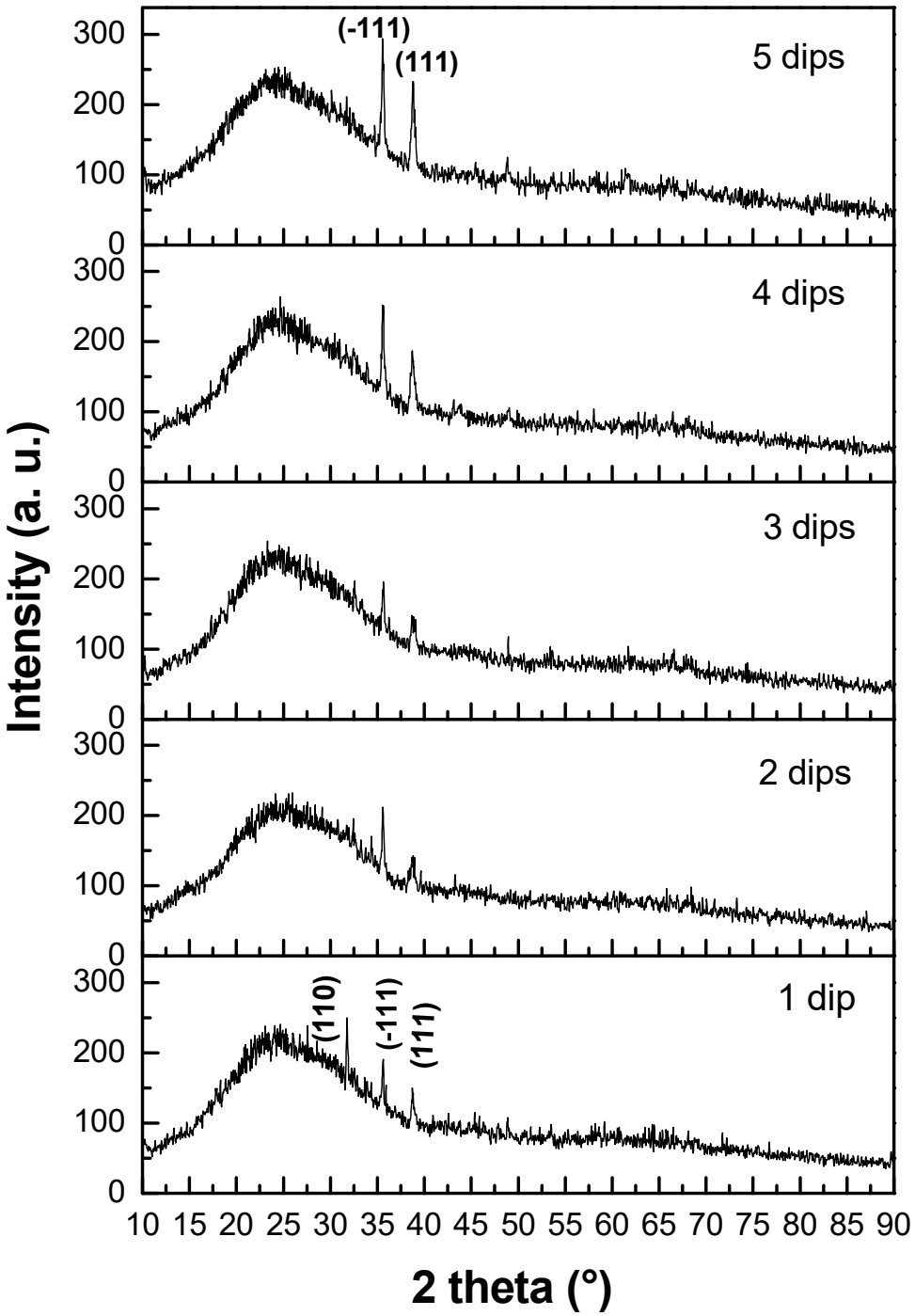

Fig. 2. X-ray diffraction patterns for the CuO thin films as afunction of thenumber dips.

[DOI: 10.22068/ijmse.2582]

The calculated values of grain size are listed in Table 2. As we can see, the average crystal-lites size deceases from 30.72 nm to 26.58 nm with the increase of the thickness which is probably due to the increased growth velocity and/or the viscosity of the solution precursor as suggested by C. Euvananont et al. [27]. The obtained values of grains sizeare in good agreement with those reported by other research [28, 29].

The micro-strain results from the geometric mismatch at inter-phase boundaries (misfit), and between crystalline lattices of films and substrate affects the film structure and hence its properties. The micro-strain (Ɛ) values of CuO films are calculated from the values of the full width at half-maximum (FWHM) in radians of the two peaks (-111) and (111) by using the following formula [21]:

$$\varepsilon = \frac{\beta \cos\theta}{4} \qquad (6)$$

The calculated values of the micro-strain are listed in Table 2. It can be seen that they varied inversely with grain size and the intensity of the XRD peaks. The change in film thickness as the number of dips rises affects the grain size; which is accompanied by a change in the grain boundaries. As a result, the micro-strain changes within the grains in the film.

3.3. Optical properties

The optical transmittance spectra of CuO thin films were recorded as a function of the wavelength in Ultra Violet-Visible and Near Infra Red regions (300-1500). The relevant da-ta are illustrated in Fig3. The transparency of the films increases with the increase of the thickness from 28(%) for 1 layer until it reaches 47(%) for 3 dips in the UV-Vis region, then it decreases. It is remarkable that between 300 and 350 nm, a strong absorption occurs due to the transition of electrons from the valence band to the conduction band.

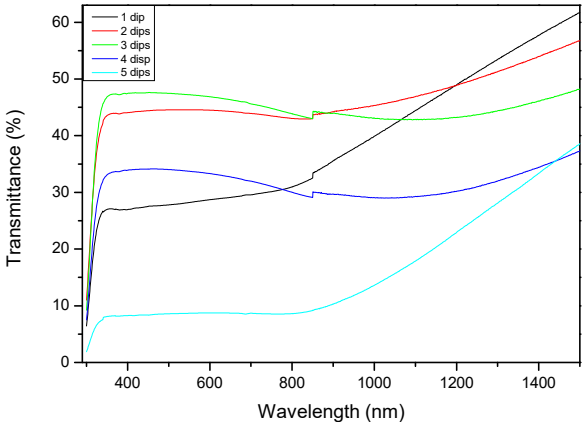

Fig. 3. The optical transmittance spectra of the obtained films of CuO elaborated with various thicknesses.

The band gap and Urach tail energies of our films are obtained using equations 3, and 4 respectively. The band gap value increases from 3.80 to 3.88 eV with the increase of number of the dips from 1 to 3 and, then decreases to reach 3.70 eV for 5 dips. The evolution of the band gap energy is attributed; in one hand, to the change in the film crystallinty, and; by the band tails states (or Urbach energy E00) on the other hand. In fact, the two phases (-111) and (111) coexist and compete; and the average grain size decreases till 4 dips then it in-creases slightly.

The variation of the band gap is inversely correlated to the (111) phase grain size, and to the Urbach tail energy thus diminishing the energy distance between the valence and conduction bands.

Table 2. Some structural properties of the deposited copper oxide thin films.

Sample	Phase	2θ(°)	Plane	D (nm)	D_{moy} (nm)	Strain *10^{-4}	$Strain_{moy}$* 10^{-4}
1 dip	CuO	31.7789	(110)	56.60	56.60	6.1223	6.1223
		35.6318 38.7390	(-111) (111)	33.42 28.01	30.72	0.1038 0.1239	0.1139
2 dips	CuO	35.6085 38.7928	(-111) (111)	39.88 18.89	29.34	8.6989 0.1837	4.4413
3 dips	CuO	35.6266 38.8034	(-111) (111)	37.43 17.71	27.57	9.2683 0.1959	4.7321
4 dips	CuO	35.6260 38.7500	(-111) (111)	32.84 20.32	26.58	0.1056 0.1707	0.1382
5 dips	CuO	35.5455 38.8000	(-111) (111)	31.98 23.52	27.75	0.1085 0.1475	0.1280

[DOI: 10.22068/ijmse.2582]

The calculated band gap energies are higher than those re-ported in reference [15] where the band gaps are in the range 1.9 - 2.10 eV depending on the Cu_2O or CuO film crystal type composition. The band gaps increase in our case can be attributed to quantum confinement effect [25, 26] due to the nanometric grains size, which it is apparent from the blue shift of the absorption edge, compared to the bulk oxide. A blue shift is observed in the CuO films obtained with high concentration solution (1.5 mol/l) which gives more copper to the film. These films were annealed for sufficient duration of time with a heating rate of 16.7°C/min which increases the rearrangement of the films network. And it changes with the band gap energy inversely and its values are between 320 to 730 meV. These tail bands result essentially from disorder and traps in the regions be-tween grains and create states in the original perfect crystal structure and hence narrows the energetic distance between valence and conduction bands therefore resulting in lower-ing the band gap. This is in good agreement with the above analysis of the films structure.

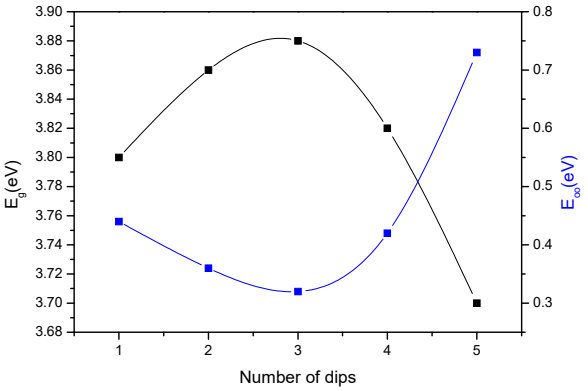

Fig. 4. Band gap energies and Urbach energies of CuO thin films asa function of thenumber of dips.

3.4. Electrical properties

The electrical resistivity is calculated using equation (5) and is illustrated in figure 5.It can be seen that the resistivity increases with increasing in the thickness and its values are in the range of tens to hundreds of (Ω.cm) as showed in figure 5. Similar behaviour with the change in the electrical resistivity has been reported by Hashim et al. [33]. This parameter is strongly related to the film's structure because of the decrease in the grain size which gives an increase of the grain boundaries and the density of charge carriers traps which reduces the mobility of charges and hence leading to higher resistivity.

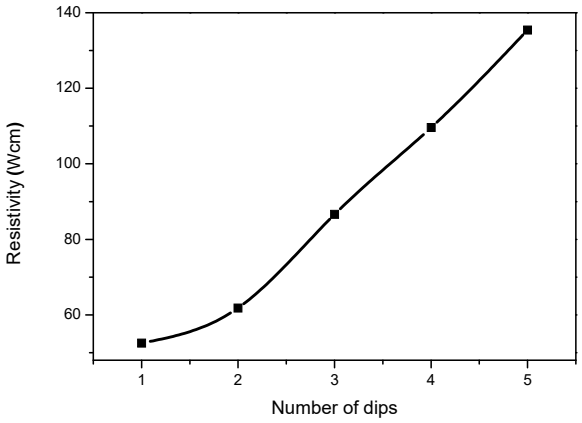

Fig. 5. The electrical resistivity of the deposited films of CuO as function of number of the dips.

4. CONCLUSIONS

Sol-gel dip coating method was used successfully to develop polycrystalline cupric oxide thin films deposited onto glass substrate. The number of the dips as an effective parameter on the physical properties was fully studied. The preferential growth orientation (-111) of monoclinic structure belongs to 2C/2 group space and the grain size decreased from 30.72 to 26.58 nm with the increase in the film thickness. The FWHM of the obtained films increased from 0.17° to 0.25° with the increase in the film thickness from 471.04 to 1219.36 (nm). Increasing the layer's number led to a decreased stress which was related to the improvement in film's crystallinity. The recorded UV-Vis spectra showed that the CuO thin dips are relatively transparent in UV-Vis region and transparent (around 65 %) in the NIR range. The band gap energies are higher than in the bulk material which may be due to the quantum confinement effect. The resistivity of the films increased from 52.52 to 135.40 Ω.cm with the increase in the film thickness. The results concludes that the obtained CuO films may be considered as potential candidates for photovoltaic applications and optoelectronic devices.

REFERENCES

[1] Gangwar, J., Gupta; B. K., and Srivastava A. K.," Prospects of Emerging Engineered

[DOI: 10.22068/ijmse.2582]

oxide nanomaterials and their Applications", J. Def. Sci., 2016, 66 (4), 323-340.

[2] Ito; T., Yamaguchi; H., and Okabe; K., "Single-crystal growth and characterization of Cu_2O and CuO", J. Mater. Sci., 1998, 3, 3555-3566.

[3] Li, J., Vizkelethy, G., Revesz, P., Mayer J., and Tu, K., "Oxidation and reduction of cop-per oxide thin films", Journal of applied physics, 1991, Vol. 69, 1020-1029.

[4] Marabelli, F., Parravicini, G. B., and Salghetti-Drioli, F., "Optical gap of CuO", Phys. Rev. B, 1995, 52, 1433–1436.

[5] Dörner, L., Cancellieri, C., Rheingans, B., Walter, M., Kägi R., Schmutz, P., Kovalenko, M. V., and Jeurgens, L. P. H., "Cost-effective sol-gel synthesis of porous CuO nanoparticle aggregates with tunable specific surface area", Scientific Reports, 2019 9,11758.

[6] Deng, G., Li, K., Zhang, G., Gu Z., Zhu, X., Wei, Y., and Wang, H., "Enhanced performance of red mud-based oxygen carriers by CuO for chemical looping combustion of methane", Applied Energy, 2019, Vol. 253, 1, 113534.

[7] Thim, G. P., Maria Oliveira, A. S., Oliveira, E. D. A., Melo, F. C. L., "Sol-gel silica film preparation from aqueous solutions for corrosion protectiona", Journal of Non-Crystalline Solids, 2000, 273, 124-128.

[8] Toupin, J., Strubb, H., Kressman, S., Artero, V., Krins, N., and Laberty-Robert, Ch., "CuO photo-electrodes synthesized by the sol-gel method for water splitting", Journal of Sol-Gel Science and Technology, 2019, 89:255–263.

[9] Zhang, W., Ma, G., Gu, H., Yang, Z., and Cheng, H., "A new lithium-ion battery: CuO na-norod array anode versus spinel LiNi0. 5Mn1. 5O4 cathode", Journal of Power Sources, 2015, 273, 561-565.

[10] Li, D., Zu, X., Ao, D., Tang, Q., Fu, Y. Q., Guo, Y., Bilawal, K., Faheem, M. B., Li, L., Li, S., and Tang, Y., "High humidity enhanced surface acoustic wave (SAW) H_2S sensors based on sol-gel CuO films", Sensors and Actuators B. chemical, 2019, 294, 55-61.

[11] Zeggar, M. L., Bourfaa, F., Adjimi, A., Boutbakh, F., Aida, M. S., and Attaf, N., "CuO thin films deposition by spray pyrolysis: influence of precursor solution properties", Interna-tional Journal of Mathematical, Computational, Physical, Electrical and Computer Engi-neering, 2015, 9, N° 10, 489-493.

[12] Ogwu, A. A., Darma, T. H., and Bouquerel, E., "Electrical resistivity of copper oxide thin films prepared by reactive magnetron sputtering", Journal of Achievements in Materials and Manufacturing Engineering 2007, 24. 172-177.

[13] Keikhaei, M., and Ichimura, M., "Fabrication of Copper Oxide thin films by galvanostat-ic deposition from weakly acidic solutions", Int. J. Electrochem. Sci., 2018, 13, 9931 – 9941.

[14] Lamri, Z. M., Chabane, L., Aida, M. S., Attaf, N., and Zebbar, N., "Solution flow rate in-fluence on properties of copper oxide thin films deposited by ultrasonic spray pyrolysis", Materials Science in semiconductor processing, 2015, 30, 645-650.

[15] Ray, S. C., "Preparation of copper oxide thin film by the sol–gel-like dip technique and study of their structural and optical properties", Solar Energy Materials and Solar Cells, 2001 68(3-4), 307–312.

[16] Al-Khanbashi, H. A., Shirbeeny, W., Al-Ghamdi, A. A., and Bronstein, L. M., "Spectro-scopic ellipsometry of $Zn_{1-x}Cu_xO$ thin films based on a modified sol-gel dip-coating tech-nique", Spectrochimica Acta Part A: Molecular and Biomolecular Spectroscopy, 2014, 118, 800-805.

[17] Prabeesh, P., Saritha, P., and Selvam, I. P., "Fabrication of CZTS thin films by dip-coating technique for solar cell applications", Materials Research Bulletin, 2017, 86, 295-301.

[18] Aswathy, B. R., Vinay, K., Arjun, M., and Manoj, P. K., "Deposition of tin oxide thin film by sol-gel dip-coating technique and its characterization" AIP Conference Proceedings 2019, 2162, 020134.

[19] Cao, H., Zhou, Z., Yu, J., and Zhou, X.," DFT study on structural, electronic, and optical properties of cubic and monoclinic CuO", J. Comput. Electron., 2018, 17, 21–28.

[DOI: 10.22068/ijmse.2582]

[20] Al-Maiyaly, B. K. H., Khudayer, I. H., and Ibraheim, A. J., " Effect of ambient oxidation on structural and optical properties of copper oxide thin films", International Journal of Innovative Research in Science, Engineering and Technology, 2014, 3, 2014, 3, 8694- 8701.

[21] Nwanna, E. C., Imoisili, P. E., Bitire, S. O., and Jen, T. , "Biosynthesis and Fabrication of Copper Oxide Thin Films as a P-Type Semiconductor for Solar Cell Applications", Coat-ings (2021), N° 11, 1545-1558.

[22] Li, Y., Liang, J., Tao, Z., and Chen, J., "CuO particles and plates: synthesis and gas-sensor application", Materials Research Bulletin, 2008, 43, 2380-2385.

[23] Morales, J., Sanchez, L., Martin, F., Ramos-Barrado, J. R., and Sanchez, M., "Nanostruc-tured CuO thin film electrodes prepared by spray pyrolysis: a simple method for enhancing the electrochemical performance of CuO in lithium cells", Electrochimica Acta, 2004, 49, 4589–4597.

[24] El-Kodadi, M., Malek, F., Ramdani, A., Eddike, D., and Tillard, M., "Synthesis, Crystal structure and catecholase activity of [N, N-bis(3,5-dimethylpyrazol-1-ylmethyl)-1-hydroxy-4-aminobutane] copper(II) dichloride". J. Mar. Chim. Heterocycl., 2004, 61 (3/1), 45-52.

[25] Attouche, H., Rahmane, S., Hettal, S., and Kouidri, N., "Precursor nature and molarities effect on the optical, structural, morphological, and electrical properties of TiO_2 thin films deposited by spray pyrolysis", Optik, 2020, 203,163985-163993.

[26] Euvananont, C., Junin, Inpor, Limthongkul, C., K., and Thanachayanont, P. C., "TiO_2 optical coating layers for self-cleaning applications", Ceramics International, 2008, 34, 1067–1071.

[27] Abdelkrim, A., Rahmane, S., Ouahab, A., Abdelmalek, N., Gasmi, B., "Effect of solution concentration on the structural, optical and electrical properties of SnO_2 thin films pre-pared by spray pyrolysis", Optik, 2016, 127, 2653–2658.

[28] Kayani, Z. N., Ali, Y., Kiran, F., Batool, I., Butt, M. Z., Umer, M., Riaz, S., and Naseem, S., "Fabrication of Copper Oxide Nanoparticles by Sol-gel Route", Materials Today: Pro-ceedings, 2015, 2, 10, Part B, 5446-5449.

[29] Akgul, F. A., Akgul, G., Yildirin, N., Unalan, H. E., and Turan, R., "Influence of thermal annealing on microstructural, morphological, optical properties and surface electronic structure of copper oxide thin films", Materials chemistry and physics, 2014,147, 987-995.

[30] Rahmane, S., Djouadi, M. A., Aida, M. S., and Barreau, N., "Oxygen effect in radio fre-quency magnetron sputtered aluminum doped zinc oxide films", Thin Solid Films, 2014 562, 70–74.

[31] Sakka, S., Handbook of sol-gel sciences and technology: Processing, Characterization and Applications, Springer, 2005, Vol. II, 397.

[32] Moumen, A., Hartiti, B., Thevenin, P., and Siadat, M., "Synthesis and characterization of CuO thin films grown by chemical spray pyrolysis", Opt Quant Electron, 2017, 49 (2), 69-81.

[33] Hashim, H., Shariffudin, S. S., Saad, P. S. M., and Ridah, H. A. M., "Electrical and opti-cal properties of copper oxide thin films by sol-gel technique" Materials Science and Engi-neering, 2015, 99-108.

[DOI: 10.22068/ijmse.2582]